nature neuroscience

In vivo time-lapse imaging shows dynamic oligodendrocyte progenitor behavior during zebrafish development

Brandon B Kirby[1,3], Norio Takada[1,3], Andrew J Latimer[1], Jimann Shin[1], Thomas J Carney[2,4], Robert N Kelsh[2] & Bruce Appel[1]

Myelinating oligodendrocytes arise from migratory and proliferative oligodendrocyte progenitor cells (OPCs). Complete myelination requires that oligodendrocytes be uniformly distributed and form numerous, periodically spaced membrane sheaths along the entire length of target axons. Mechanisms that determine spacing of oligodendrocytes and their myelinating processes are not known. Using *in vivo* time-lapse confocal microscopy, we show that zebrafish OPCs continuously extend and retract numerous filopodium-like processes as they migrate and settle into their final positions. Process remodeling and migration paths are highly variable and seem to be influenced by contact with neighboring OPCs. After laser ablation of oligodendrocyte-lineage cells, nearby OPCs divide more frequently, orient processes toward the ablated cells and migrate to fill the unoccupied space. Thus, process activity before axon wrapping might serve as a surveillance mechanism by which OPCs determine the presence or absence of nearby oligodendrocyte-lineage cells, facilitating uniform spacing of oligodendrocytes and complete myelination.

Rapid conduction of nerve impulses in vertebrates requires that most large-diameter axons be wrapped by myelin. In the CNS, myelin sheaths are formed by oligodendrocytes, one of the major classes of glial cells[1,2]. During development, discrete subpopulations of neural precursors give rise to OPCs. OPCs proliferate and migrate from their origins, eventually becoming uniformly distributed throughout the gray and white matter of the brain and spinal cord[3]. During late embryogenesis and early postnatal life, many OPCs stop dividing and differentiate as oligodendrocytes, which extend fine membrane processes that wrap axons. Each oligodendrocyte can wrap numerous axons, and each axon is ensheathed by periodically spaced processes extending from multiple oligodendrocytes. Uniform and periodic spacing of myelin sheaths on axons is a critical feature of saltatory conduction, but whether spacing is determined by OPCs or positional cues within axons is unknown.

To investigate behavior of OPCs as they migrate and make contact with axons *in vivo*, we created transgenic zebrafish that express fluorescent proteins in oligodendrocyte-lineage cells and performed time-lapse imaging during normal development and after laser microsurgical removal of nearby cells. Our data establish three key points. First, OPCs constantly remodel numerous filopodium-like processes as they migrate and for many hours before they wrap axons. Second, OPCs often retract processes and change direction of migration after making contact with a neighboring OPC. Third, OPCs can divide and migrate to replace nearby oligodendrocyte-lineage cells removed by laser microsurgery. These results raise the possibility that OPCs survey their environments by filopodial activity and adjust their migration and division according to the density and distribution of nearby OPCs and oligodendrocytes. Density-dependent regulation of migration and division ensures a uniform distribution of oligodendrocytes, facilitating uniform myelination.

In mice, genetically ablated subpopulations of OPCs are rapidly replaced by nearby cells, suggesting that OPCs compete for space[4]. In humans, OPCs seemingly divide and migrate to replace oligodendrocytes lost from disease or injury[5]. Our data point toward filopodium-based surveillance a mechanism that regulates myelination and, possibly, remyelination.

RESULTS

Migrating OPCs rapidly remodel filopodium-like processes

The transgenic line *Tg(nkx2.2a:megfp)* expresses a membrane-tethered enhanced green fluorescent protein (mEGFP) under control of *nkx2.2a* regulatory sequences carried on a bacterial artificial chromosome (BAC)[6]. The transgene expresses EGFP in a pattern similar to *nkx2.2a* RNA, marking a subset of oligodendrocyte-lineage cells (data not shown). To examine spinal cord OPC behaviors, we mounted *Tg(nkx2.2a:megfp)* embryos on their sides and performed time-lapse imaging using spinning disc confocal microscopy from 36 h post-fertilization (hpf), when OPCs are first specified in ventral spinal cord of zebrafish, to 72 hpf, when axon wrapping is initiated (**Fig. 1** and

[1]Department of Biological Sciences, Vanderbilt University, 465 21st Avenue South, Nashville, Tennessee 37232, USA. [2]Centre for Regenerative Medicine, Department of Biology and Biochemistry, University of Bath, Bath BA2 7AY, UK. [3]These authors contributed equally to this work. [4]Present address: Spemann Laboratories, Max-Planck-Institut fur Immunobiologie, Stuebeweg 51, Freiburg D-79108, Germany. Correspondence should be addressed to B.A. (b.appel@vanderbilt.edu).

Received 14 September; accepted 24 October; published online 12 November 2006; doi:10.1038/nn1803

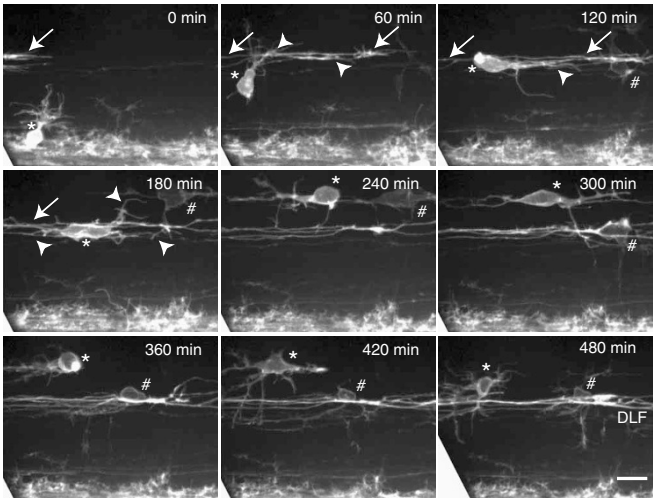

Figure 1 OPC migration in zebrafish spinal cord. Frames were captured from a 36-h time-lapse sequence. Images were obtained from the side of the spinal cord of a *Tg*(*nkx2.2a:megfp*) larva, with dorsal up and anterior left. The 0-min time point is from approximately the 40-hpf stage. Times shown in upper right corners represent time elapsed after the start of the sequence. Two OPCs are marked by * and #. Axons migrating in the dorsal longitudinal fascicle (DLF) are indicated by arrows and OPC processes by arrowheads. Scale bar equals 22 μm.

Supplementary Video 1 online). Migrating OPCs formed numerous, highly branched filopodium-like processes that typically, but not exclusively, extended in the direction of migration. The *Tg*(*nkx2.2a:megfp*) transgene marks axons that descend from the hindbrain through the dorsal longitudinal fascicle (DLF). OPCs appeared to make contact with these axons and generally stopped their dorsalward movement at the DLF. Occasionally OPCs continued dorsally but returned to the DLF. Once at the DLF, OPC process extension and retraction persisted for several hours until the cells began to wrap axons and some OPCs continued to adjust their positions with longitudinal movements.

Time-lapse imaging showed that OPC process activity was highly dynamic during migration. To quantify process motility, we collected images at 2-min intervals and measured changes in process length. We found that the same process could extend, retract and form new branches within a few minutes (**Fig. 2a**,**b**). An OPC could both extend and retract different processes at the same time, but extension and retraction were not necessarily balanced (**Fig. 2c**). The velocity of extension and retraction were similar, averaging from about 4.2–7.4 μm for each 2-min period for four individual processes, but were highly variable, ranging from <1 μm to >13 μm (**Fig. 2d**).

Time-lapse imaging also showed that although OPCs had a net dorsal movement, they frequently changed direction to move ventrally, anteriorly and posteriorly (**Fig. 3a** and **Supplementary Video 1**). OPCs that migrated anteriorly or posteriorly were usually close to DLF axons. OPCs did not migrate at consistent rates but instead moved intermittently. Among the 18 cells we traced, none followed a straight path, and no two paths were the same. The total distance traveled by individual OPCs was variable, ranging from 43–253 μm (**Fig. 3b**). OPCs occasionally retracted all their processes and divided (**Fig. 3c** and **Supplementary Video 1**). These cells were usually close to the DLF and always divided in the longitudinal plane. In every case, sister OPCs subsequently migrated away from each other.

We noticed that process retraction and alteration of migratory paths often occurred after apparent contacts between neighboring OPCs (**Fig. 4a** and **Supplementary Video 1**). To examine interactions between neighboring cells more carefully, we marked OPCs with different-color fluorescent proteins by injecting *Tg*(*nkx2.2:megfp*)

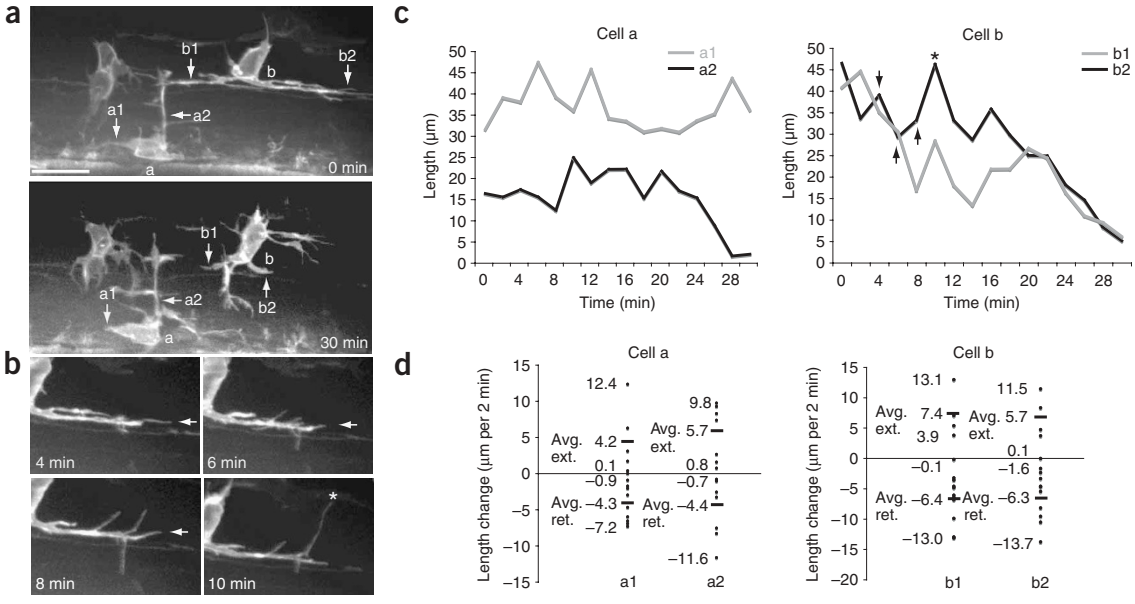

Figure 2 OPC processes are rapidly and extensively remodeled. Images were captured from a time-lapse sequence of an approximately 60-hpf *Tg*(*nkx2.2a:megfp*) larva; dorsal is up and anterior is left. (**a**) First and last images of a 30-min time-lapse sequence. Two processes (1 and 2) for each of two cells (a and b) are indicated by arrows. (**b**) Six-minute image sequence for process b2. Arrow indicates retracting process, and asterisk marks formation of a new branch. (**c**) Graphs showing process length changes during the 30-min imaging sequence. Arrows and asterisk correspond to those in **b**. (**d**) Graphs showing velocity of process extensions and retractions. Extensions are shown as positive numbers and retractions as negative numbers. The average extension ('avg. ext.') and average retraction ('avg. ret.') are indicated for each process. Scale bar equals 15 μm.

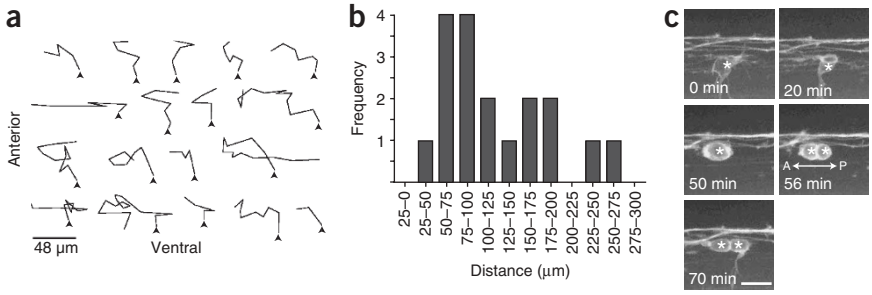

Figure 3 OPC migration is variable in direction and distance. (**a**) Tracings of migratory paths of 18 OPCs. Each trace is oriented so that ventral is to the bottom and anterior to the left. Arrowheads indicate starting point of each cell. (**b**) Graph showing total distances traveled by individual OPCs. Distances are split into 25-μm bins, and the number of OPCs in each category is plotted on the *y*-axis. (**c**) Images captured from a time-lapse sequence showing an OPC (asterisk) retracting its process, rounding up and dividing in the anteroposterior axis to produce two daughter OPCs. Scale bar for **c** equals 15 μm.

embryos with the plasmid *p7.2sox10:mrfp*, which drives expression of membrane-tethered monomeric red fluorescent protein (RFP) under control of *sox10* regulatory DNA[7]. Injected plasmids were distributed mosaically, resulting in a mixture of mEGFP$^+$ mRFP$^+$, mEGFP$^+$ mRFP$^-$ and mEGFP$^-$ mRFP$^+$ OPCs. This demonstrated extensive overlap and interdigitation at the process terminals of neighboring OPCs (**Fig. 4b** and **Supplementary Video 2** online). Overlapping terminals were constantly remodeled and gradually withdrew from each other to occupy largely nonoverlapping territories. Thus, process activity and migration seem to be influenced by signals, perhaps mediated by contact, that pass between OPCs.

OPCs divide and migrate to replace nearby ablated cells

Oligodendrocytes might be regularly spaced because OPC process activity functions as a surveillance mechanism to recognize the presence or absence of nearby oligodendrocyte-lineage cells. Accordingly, OPCs should divide and migrate to fill territories unoccupied by other OPCs, producing a uniform distribution. We tested this using a laser to ablate oligodendrocyte-lineage cells expressing a cytosolic EGFP driven by *olig2* regulatory DNA in *Tg*(*olig2:egfp*) larvae[8]. We ablated cells in 4-d-post-fertilization (dpf) larvae, 1 d after initiation of axon wrapping, because little OPC division and migration occurs normally at that time (see below). A small amount of cell debris was evident immediately after ablation (**Fig. 5a**,**b**) showing that the targeted cells were effectively killed. We confirmed that oligodendrocyte-lineage cells were eliminated by ablating cells on one side of the spinal cord and labeling transverse sections with Sox10 antibody (**Fig. 5c**). In one series of experiments, ablated sides had 12 EGFP$^+$ Sox10$^+$ cells, compared with 54 on control sides ($n = 3$ larvae). By contrast, EGFP$^+$ cells did not die when we ablated neural cells next to them, suggesting that the laser did not create extensive damage outside the targeted cell (data not shown). Next, we ablated all oligodendrocyte-lineage cells within a five-hemisegment region of the dorsal trunk spinal cord. One day later, the number of EGFP$^+$ cells within the ablated region was about 50% of neighboring control hemisegments (**Fig. 5d**). The number of OPCs in the ablated region continued to increase, reaching about 70% of the number of neighboring control hemisegments by 4 d after ablation. When we ablated a single neural cell next to each OPC and oligodendrocyte within a four-hemisegment region at 4 dpf ($n = 13$ larvae), EGFP$^+$ cell number did not differ from control hemisegments during the following 2 d, indicating that OPCs did not proliferate in response to general cell damage. We then reasoned that ablated oligodendrocyte-lineage cells could be replaced by OPCs from nearby unablated regions of spinal cord, by ventral neural precursors or by dorsal neural precursors that were recently shown to produce a small number of OPCs in mouse[9–12]. To distinguish between these possibilities, we performed time-lapse imaging after laser ablation. Within 3 h, EGFP$^+$ OPCs began to migrate into the ablated region from nearby anterior, posterior and ventral regions (**Fig. 5e** and **Supplementary Video 3** online). At the same time, a larger percentage of OPCs divided compared with control larvae. During time-lapse sequences of control larvae, 16% of dorsal EGFP$^+$ oligodendrocyte-lineage cells migrated and divided (two larvae, imaged for 16 and 21.5 h, 18.75 h average), whereas in ablated larvae, 44% of the cells migrated and divided (three larvae, imaged at 11.5, 15 and 20 h; 15.5 h average). In time-lapse imaged experimental larvae, all EGFP$^+$ cells that occupied the ablated region originated as nearby OPCs and did not arise *de novo* from ventral or dorsal precursors (**Fig. 5e**).

To examine more closely the behavior of OPCs after ablation of nearby cells, we performed experiments using *Tg*(*nkx2.2a:megfp*) larvae. Because it is difficult to see cell bodies at 4 dpf using this transgene, we ablated cells between 50–60 hpf, before axon wrapping normally begins. Fewer than 2 h after ablation, nearby OPCs in both dorsal and ventral spinal cord began to remodel their processes so that the majority extended toward the ablation site (**Fig. 5f** and **Supplementary Video 4** online). Within 5 h, the site was filled with OPCs that

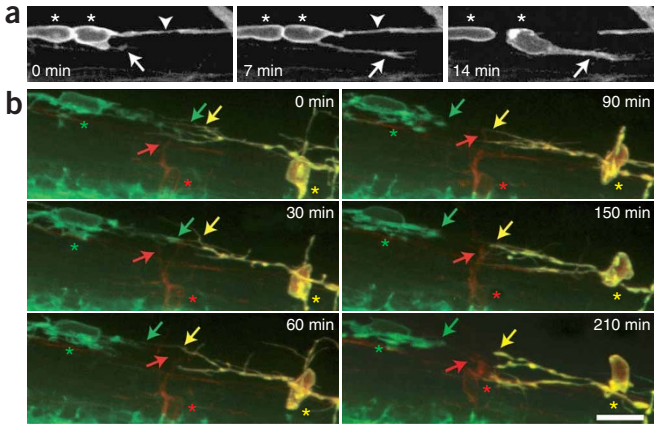

Figure 4 OPC processes retract after contact. (**a**) Images captured from time-lapse sequence showing two newly divided sister OPCs (asterisks). At 0 min in the sequence, one OPC extended a secondary process (arrow) soon after making contact with a process from an OPC outside the field of view (arrowhead). At 7 min, the secondary process had extended. By 14 min, the primary process had retracted, and the OPC began to migrate behind the secondary process. (**b**) Images captured from time-lapse sequence showing interactions of three OPCs. At 0 min in the sequence, a mEGFP$^+$ mRFP$^-$ OPC (green asterisk) extended a process (green arrow) that interdigitated with a process from a mEGFP$^+$ mRFP$^+$ OPC (yellow asterisk and yellow arrow). These processes withdrew from each other over time, while a mEGFP$^-$ mRFP$^+$ OPC extended a process (red asterisk and red arrow) and migrated dorsally to fill the vacated space. Scale bar equals 15 μm.

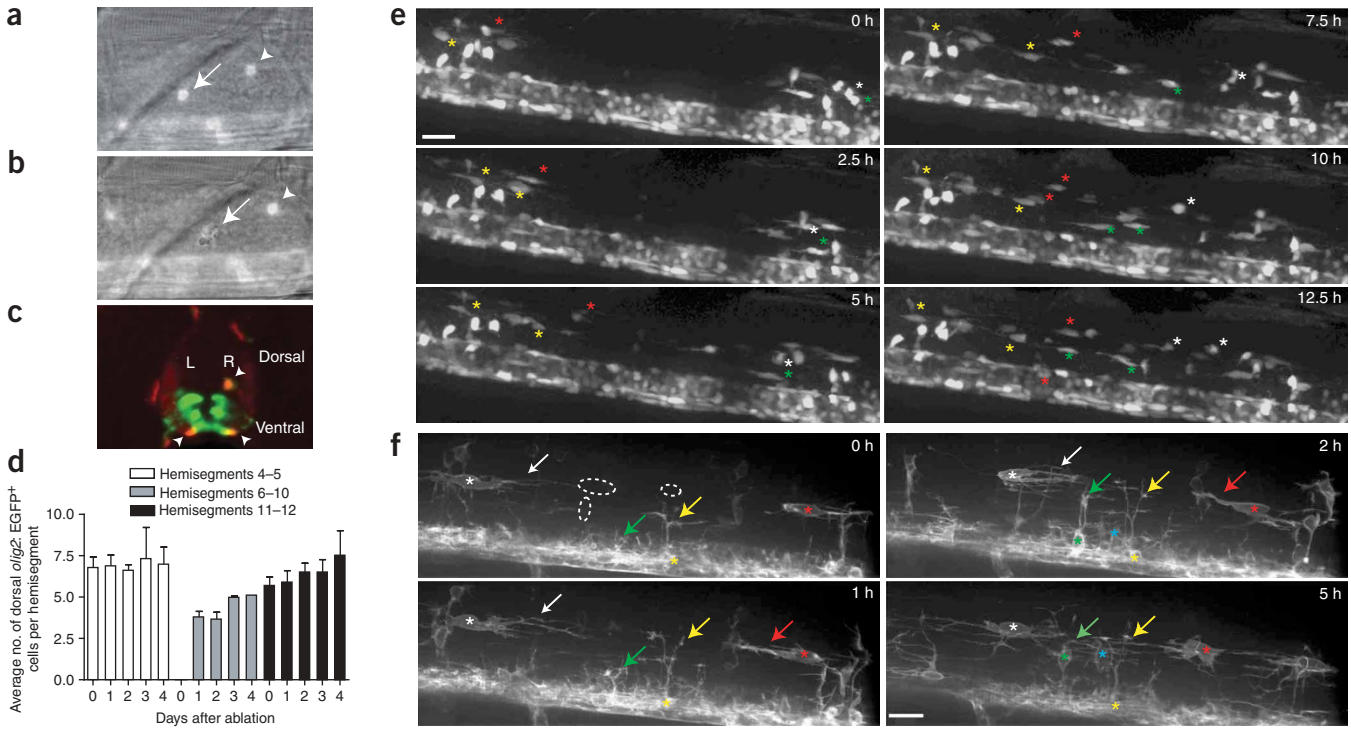

Figure 5 OPCs divide and migrate to replace ablated cells. (**a**,**b**) Images of spinal cord of a *Tg*(*olig2:egfp*) larva before and after laser ablation. Arrow and arrowhead mark ablated and nonablated OPCs, respectively. Dorsal is up. (**c**) Transverse section of *Tg*(*olig2:egfp*) larva in which OPCs were ablated in the dorsal left spinal cord. Arrowheads mark EGFP$^+$ Sox10$^+$ OPCs in ventral and dorsal right spinal cord. (**d**) Quantification of dorsal oligodendrocyte-lineage cells after ablation at 4 dpf (0 d after ablation) and each day until 4 d after ablation. White and black bars show average number of dorsal EGFP$^+$ cells in control hemisegments 4–5 and 11–12, respectively, which border ablated hemisegments 6–10, represented by gray bars. Error bars indicate s.e.m. For ablated versus control hemisegment cell counts, $P < 0.05$ for 0–2 d after ablation and $P > 0.05$ for 3 and 4 d after ablation. (**e**) Time-lapse images after ablation. Dorsal is up. Two OPCs on either side of the ablated region are marked by asterisks. Each OPC migrated into the ablated region and divided a single time. Sister OPCs are marked by asterisks of the same color. Scale bar equals 48 μm. (**f**) Time-lapse images after ablation of dorsal OPCs in a 3-dpf *Tg*(*nkx2.2a:megfp*) larva. The positions of the ablated cells are outlined in the first frame. Dorsal and ventral OPCs that extended processes and migrated into the ablation site are marked by asterisks and arrows. Scale bar equals 24 μm.

migrated longitudinally from dorsal spinal cord and dorsally from ventral spinal cord. Within 12 h, newly migrated OPCs began to wrap axons. Together with the above data, these observations show that OPCs can rapidly adjust their filopodium-like processes, migratory activities and rate of division in response to loss of nearby oligodendrocyte-lineage cells.

DISCUSSION

Uniform myelination requires uniform distribution of oligodendrocytes in sufficient number to wrap the entire length of all target axons. Because oligodendrocyte-lineage cells arise as proliferative progenitors from spatially restricted subsets of neural precursors, key influences of oligodendrocyte distribution include OPC migration and division[13]. Secreted growth factors regulate both OPC motility and division rate, but the mechanisms by which oligodendrocytes are uniformly distributed are unclear[14]. As oligodendrocyte-lineage cells develop, they produce numerous fine membrane processes that eventually wrap axons[1,2]. Our data provide evidence that OPC process activity influences oligodendrocyte spacing.

One of the most notable features of the development of oligodendrocytes is their formation of extensive membrane processes. Distinct process morphologies are evident in fixed tissues and cell culture, and these seem to represent progressive oligodendrocyte maturation from premyelinating to myelinating states[1,2]. Process remodeling has been inferred previously from examination of antibody-labeled oligodendrocyte-lineage cells in fixed thick sections of mouse brains[15] and observed directly by time-lapse imaging of cultured oligodendrocytes[16]. However, these activities are associated with apparently post-mitotic, nonmigratory cells and are assumed to reflect a mechanism for axon identification and contact. By contrast to the elaborate morphologies of more mature cells, migrating OPCs in cell culture or cultured tissue slices usually appear to have unipolar or bipolar morphologies[17–20]. Consequently, we were surprised by the number and dynamic activity of OPC processes during migration in zebrafish. Our imaging shows that zebrafish OPCs can be unipolar or bipolar but that these are very transient states, and the cells frequently form more numerous processes that project in different directions. Process extension, retraction and higher-order branching are interrupted only when OPCs divide and otherwise occur continuously until the cells settle into their final positions and begin to wrap axons. Thus, OPC process activity may be more extensive than previously appreciated. Although morphological differences in OPCs could reflect species differences, we think an alternative explanation is that various labeling methods produce different impressions of OPC shape and behavior. In fact, from examination of the *Tg*(*olig2:egfp*) transgenic line, which expresses a cytosolic form of EGFP, we had previously concluded that migrating OPCs are bipolar in zebrafish[8]. By examining in this study a new line that expresses a membrane-localized EGFP, we have been able to see processes that were not visible with cytosolic EGFP.

Dynamic process activity could serve as a mechanism for OPCs to survey their environments for extracellular cues. Consistent with this idea, structures similar to axonal growth cones, which are associated with signal reception, often form at the process tips of cultured oligodendrocyte-lineage cells[18,19,21], and they are evident in our *in vivo* time-lapse sequences. Numerous secreted and contact-mediated signals are implicated in regulation of OPC migration and proliferation[3,22]. For example, Netrin-1, a secreted molecule that can either attract or repel axons[23], can repel OPCs *in vitro*[24–26]. In mouse embryos, ventral midline cells close to the origin of OPCs express Netrin-1, whereas OPCs express the Netrin receptors DCC and Unc5h1 (ref. 25), and OPCs do not disperse from the ventral spinal cord of mutant mice lacking functional Netrin-1 or DCC[20,25]. Secreted platelet-derived growth factor-A (PDGF-A) also promotes OPC migration, as well as proliferation *in vitro*[19,27–31]. Transgenic mice that overexpress PDGF-A produce excess OPCs[32], and PDGF-A–deficient mice form greatly reduced numbers of OPCs and oligodendrocytes[32,33], establishing a critical role for this growth factor. Oligodendrocyte-lineage cells express distinct integrins (cell surface receptors for extracellular matrix ligands) as they mature[34,35], and these have been functionally linked with migration, proliferation and differentiation[17,36]. Integrins can influence growth factor signaling and consequently might help regulate transition of OPC migratory, proliferative and differentiative behaviors in response to broadly distributed signals[14]. However, mechanisms that ensure uniform spacing of oligodendrocytes, leading to uniform and complete myelination, remain unknown.

Observations from our time-lapse imaging raise the possibility that the spacing of oligodendrocytes is influenced by contact-mediated signaling between OPCs as they migrate and divide to populate the neural tube. Dorsally migrating OPC paths are not straight, as would be predicted if they were simply moving down a Netrin chemorepellent gradient, but instead are highly variable, with OPCs frequently pausing and changing direction to move anteriorly, posteriorly and even ventrally. OPCs migrating in cell culture and tissue slices show similar stop-and-go movements[18,20]. We found that OPC processes often seem to withdraw after contact with a nearby process, suggesting that they repel one another, and that contact frequently precedes a change in the trajectory of OPC migration. Consequently, during development, OPCs might divide and migrate to fill space not occupied by other OPCs, eventually achieving a uniform distribution.

When subsets of OPCs are genetically ablated in mice, they are rapidly replaced, suggesting that OPCs compete for space[4]. Similarly, experimental demyelination in rodents is followed by elevated rates of OPC division[37,38], and demyelinated lesions of individuals with multiple sclerosis appear to be populated by immature oligodendrocyte-lineage cells[39–43]. Because OPC number seems to be finely tuned by the level of growth factor[32,44], loss of OPCs might increase available PDGF, leading to an elevated proliferative response by remaining OPCs[44]. Additional regulatory mechanisms might involve contact between OPCs. OPCs cultured at different densities give rise to similar numbers of oligodendrocyte-lineage cells after several days because cells at low density divide more often than those at high density[45]. OPC proliferation in this system is not limited by PDGF but instead seems to be restricted by cell contact. By subtly changing oligodendrocyte density *in vivo* using cell ablation, we have found that nearby OPCs divide and migrate to rapidly fill the vacated space. This is consistent with the possibility that OPC migration and division are normally limited by contact inhibition, although we cannot rule out the possibility that ablation releases an attractive and mitogenic signal. Contact inhibition of proliferation via, for example, activation of receptor tyrosine phosphatases by molecules on the surface of adjacent cells, is an important mechanism of growth control[46], but molecules that might mediate it in OPCs have not been described.

Dynamic process activity, surveillance and cell-cell interaction might be general features of vertebrate glial cells. *In vivo* time-lapse imaging demonstrates that resting microglia constantly extend and retract fine processes that can be rapidly oriented toward nearby lesions[47]. Astrocytes also rapidly remodel processes[48], which might mediate dynamic interactions with synapses and blood vessels. Processes of neighboring microglia seem to repel one another[47], and processes of astrocytes terminate close to one another but do not intermingle[49]. Thus, glial process activity might serve both to mediate cell-cell interactions that influence glial cell number and spacing and to facilitate glial cell functions.

METHODS

Fish breeding and maintenance. Embryos were produced by pairwise matings, raised at 28.5 °C in egg water or embryo medium (EM) and staged according to hours post-fertilization (hpf), days post-fertilization (dpf) and morphological criteria. *Tg*(*olig2:egfp*) (ref. 8) and *Tg*(*nkx2.2a:megfp*) (ref. 6) fish were used for this study.

Plasmid construction and DNA injection. To construct *p7.2sox10:mrfp*, a 7.2-kb genomic fragment of *sox10* (ref. 7) was subcloned into the *Xba*I and *Sal*I sites of a modified pBluescript II plasmid that carried I-*Sce*I recognition sequences flanking both ends of the multiple cloning site. cDNA encoding membrane-localized red fluorescent protein (mRFP) upstream of an SV40 polyadenylation signal was then cut from *pCS2:mrfp* using *Eco*RI and *Not*I and inserted downstream of the *sox10* sequence. *p7.2sox10:mrfp* plasmid was injected at the one-cell stage with I-*Sce*I (New England Biolabs) as described previously[50].

Time-lapse photomicroscopy. At 24 hpf, manually dechorionated embryos were transferred to EM containing 0.003% phenyl-thiourea to prevent formation of dark pigment and were then returned to a 28.5 °C incubator. Larvae used for imaging were anesthetized using 3-aminobenzoic acid ethyl ester, immersed in 0.8% low–melting temperature agarose and mounted on their sides in glass-bottomed 35-mm Petri dishes. Time-lapse images were captured using 20× dry (NA = 0.75) or 40× oil-immersion (NA = 1.3) objectives mounted on a motorized Zeiss Axiovert 200 microscope equipped with a PerkinElmer ERS spinning disk confocal system and heated stage and chamber to maintain embryos at 28.5 °C. *Z* image stacks were collected every 2–5 min, and three-dimensional data sets were compiled using Sorenson 3 video compression and exported using QuickTime to create movies.

Laser microsurgical cell ablation. Anesthetized larvae were mounted on their sides in 2% methylcellulose on bridged slides and viewed using a 40× water-immersion objective of a Zeiss Axioskop microscope. Hemisegment positions were determined using adjacent somite boundaries as landmarks. Dorsally migrated EGFP$^+$ or mEGFP$^+$ oligodendrocyte-lineage cells were targeted by their fluorescence and ablated using approximately 5-s pulses of 440-nm light generated by a Photonics Micropoint Laser System. Effective ablation was demonstrated by cellular debris visible using differential interference contrast optics. In some experiments, *Tg*(*olig2:egfp*) larvae were placed individually in multiwell plates containing EM and periodically remounted, and the number of dorsal EGFP$^+$ cells within ablated hemisegments and flanking control hemisegments was determined. For time-lapse recordings, larvae were mounted and imaged as described above after ablations.

Quantification of process activity and cell migration. To measure OPC migration trajectory and distance, *Z* image stacks were compiled into composite images using Volocity. The center of each cell was identified and a line drawn to the corresponding cell at the next time point. Because soma position did not change between each time point, trajectories reflect instances where the soma moved by at least one cell diameter (~9 μm). The length of the combined line segments corresponds to the total distance each OPC migrated. To describe process activity, process length was measured at 2-min intervals.

Note: Supplementary information is available on the Nature Neuroscience website.

ACKNOWLEDGMENTS

Thanks to B. Carter for comments on the manuscript. This work was supported by US National Institutes of Health grant NS046668, National Multiple Sclerosis Foundation grant RG 3420 and a zebrafish initiative funded by the Vanderbilt University Academic Venture Capital Fund.

AUTHOR CONTRIBUTIONS

B.B.K. produced the migration data shown in **Figure 1** and **Figure 3** and the movie from which **Figure 4a** was obtained. N.T. produced the process activity data shown in **Figure 2** and **Figure 4b** and the *Tg*(*nkx2.2a:megfp*) ablation data shown in **Figure 5f**. A.J.L. performed the *Tg*(*olig2:egfp*) ablations shown in **Figure 5a–e**. J.S. created the *Tg*(*olig2:egfp*) and *Tg*(*nkx2.2:megfp*) transgenic lines. T.J.C. and R.N.K. cloned and characterized the *sox10* promoter fragment. B.A. supervised the experiments and wrote the manuscript.

COMPETING INTERESTS STATEMENT

The authors declare that they have no competing financial interests.

Published online at http://www.nature.com/natureneuroscience
Reprints and permissions information is available online at http://npg.nature.com/reprintsandpermissions/

1. Baumann, N. & Pham-Dinh, D. Biology of oligodendrocyte and myelin in the mammalian central nervous system. *Physiol. Rev.* **81**, 871–927 (2001).
2. Pfeiffer, S.E., Warrington, A.E. & Bansal, R. The oligodendrocyte and its many cellular processes. *Trends Cell Biol.* **3**, 191–197 (1993).
3. Miller, R.H. Regulation of oligodendrocyte development in the vertebrate CNS. *Prog. Neurobiol.* **67**, 451–467 (2002).
4. Kessaris, N. *et al.* Competing waves of oligodendrocytes in the forebrain and postnatal elimination of an embryonic lineage. *Nat. Neurosci.* **9**, 173–179 (2006).
5. Franklin, R.J. Why does remyelination fail in multiple sclerosis? *Nat. Rev. Neurosci.* **3**, 705–714 (2002).
6. Ng, A.N. *et al.* Formation of the digestive system in zebrafish: III. Intestinal epithelium morphogenesis. *Dev. Biol.* **286**, 114–135 (2005).
7. Dutton, K.A. *et al.* Zebrafish colourless encodes sox10 and specifies non-ectomesenchymal neural crest fates. *Development* **128**, 4113–4125 (2001).
8. Shin, J., Park, H.C., Topczewska, J.M., Mawdsley, D.J. & Appel, B. Neural cell fate analysis in zebrafish using olig2 BAC transgenics. *Methods Cell Sci.* **25**, 7–14 (2003).
9. Cai, J. *et al.* Generation of oligodendrocyte precursor cells from mouse dorsal spinal cord independent of nkx6 regulation and shh signaling. *Neuron* **45**, 41–53 (2005).
10. Vallstedt, A., Klos, J.M. & Ericson, J. Multiple dorsoventral origins of oligodendrocyte generation in the spinal cord and hindbrain. *Neuron* **45**, 55–67 (2005).
11. Fogarty, M., Richardson, W.D. & Kessaris, N. A subset of oligodendrocytes generated from radial glia in the dorsal spinal cord. *Development* **132**, 1951–1959 (2005).
12. Yue, T. *et al.* A critical role for dorsal progenitors in cortical myelination. *J. Neurosci.* **26**, 1275–1280 (2006).
13. Barres, B.A. & Raff, M.C. Control of oligodendrocyte number in the developing rat optic nerve. *Neuron* **12**, 935–942 (1994).
14. Baron, W., Colognato, H. & Ffrench-Constant, C. Integrin-growth factor interactions as regulators of oligodendroglial development and function. *Glia* **49**, 467–479 (2005).
15. Hardy, R.J. & Friedrich, V.L., Jr. Progressive remodeling of the oligodendrocyte process arbor during myelinogenesis. *Dev. Neurosci.* **18**, 243–254 (1996).
16. Kachar, B., Behar, T. & Dubois-Dalcq, M. Cell shape and motility of oligodendrocytes cultured without neurons. *Cell Tissue Res.* **244**, 27–38 (1986).
17. Milner, R., Edwards, G., Streuli, C. & Ffrench-Constant, C. A role in migration for the alpha V beta 1 integrin expressed on oligodendrocyte precursors. *J. Neurosci.* **16**, 7240–7252 (1996).
18. Schmidt, C. *et al.* Analysis of motile oligodendrocyte precursor cells *in vitro* and in brain slices. *Glia* **20**, 284–298 (1997).
19. Simpson, P.B. & Armstrong, R.C. Intracellular signals and cytoskeletal elements involved in oligodendrocyte progenitor migration. *Glia* **26**, 22–35 (1999).
20. Tsai, H.H., Macklin, W.B. & Miller, R.H. Netrin-1 is required for the normal development of spinal cord oligodendrocytes. *J. Neurosci.* **26**, 1913–1922 (2006).
21. Fox, M.A., Afshari, F.S., Alexander, J.K., Colello, R.J. & Fuss, B. Growth conelike sensorimotor structures are characteristic features of postmigratory, premyelinating oligodendrocytes. *Glia* **53**, 563–566 (2006).
22. de Castro, F. & Bribian, A. The molecular orchestra of the migration of oligodendrocyte precursors during development. *Brain Res. Brain Res. Rev.* **49**, 227–241 (2005).
23. Barallobre, M.J., Pascual, M., Del Rio, J.A. & Soriano, E. The Netrin family of guidance factors: emphasis on Netrin-1 signalling. *Brain Res. Brain Res. Rev.* **49**, 22–47 (2005).
24. Sugimoto, Y. *et al.* Guidance of glial precursor cell migration by secreted cues in the developing optic nerve. *Development* **128**, 3321–3330 (2001).
25. Jarjour, A.A. *et al.* Netrin-1 is a chemorepellent for oligodendrocyte precursor cells in the embryonic spinal cord. *J. Neurosci.* **23**, 3735–3744 (2003).
26. Tsai, H.H., Tessier-Lavigne, M. & Miller, R.H. Netrin 1 mediates spinal cord oligodendrocyte precursor dispersal. *Development* **130**, 2095–2105 (2003).
27. Zhang, H., Vutskits, L., Calaora, V., Durbec, P. & Kiss, J.Z. A role for the polysialic acid-neural cell adhesion molecule in PDGF-induced chemotaxis of oligodendrocyte precursor cells. *J. Cell Sci.* **117**, 93–103 (2004).
28. Milner, R. *et al.* Contrasting effects of mitogenic growth factors on oligodendrocyte precursor cell migration. *Glia* **19**, 85–90 (1997).
29. Noble, M., Murray, K., Stroobant, P., Waterfield, M.D. & Riddle, P. Platelet-derived growth factor promotes division and motility and inhibits premature differentiation of the oligodendrocyte/type-2 astrocyte progenitor cell. *Nature* **333**, 560–562 (1988).
30. Raff, M.C., Lillien, L.E., Richardson, W.D., Burne, J.F. & Noble, M.D. Platelet-derived growth factor from astrocytes drives the clock that times oligodendrocyte development in culture. *Nature* **333**, 562–565 (1988).
31. Richardson, W.D., Pringle, N., Mosley, M.J., Westermark, B. & Dubois-Dalcq, M. A role for platelet-derived growth factor in normal gliogenesis in the central nervous system. *Cell* **53**, 309–319 (1988).
32. Calver, A.R. *et al.* Oligodendrocyte population dynamics and the role of PDGF *in vivo*. *Neuron* **20**, 869–882 (1998).
33. Fruttiger, M. *et al.* Defective oligodendrocyte development and severe hypomyelination in PDGF-A knockout mice. *Development* **126**, 457–467 (1999).
34. Milner, R. & Ffrench-Constant, C. A developmental analysis of oligodendroglial integrins in primary cells: changes in alpha v-associated beta subunits during differentiation. *Development* **120**, 3497–3506 (1994).
35. Milner, R. *et al.* Expression of alpha vbeta3 and alpha vbeta8 integrins during oligodendrocyte precursor differentiation in the presence and absence of axons. *Glia* **21**, 350–360 (1997).
36. Blaschuk, K.L., Frost, E.E. & Ffrench-Constant, C. The regulation of proliferation and differentiation in oligodendrocyte progenitor cells by alphaV integrins. *Development* **127**, 1961–1969 (2000).
37. Redwine, J.M. & Armstrong, R.C. *In vivo* proliferation of oligodendrocyte progenitors expressing PDGFalphaR during early remyelination. *J. Neurobiol.* **37**, 413–428 (1998).
38. Levine, J.M. & Reynolds, R. Activation and proliferation of endogenous oligodendrocyte precursor cells during ethidium bromide-induced demyelination. *Exp. Neurol.* **160**, 333–347 (1999).
39. Scolding, N. *et al.* Oligodendrocyte progenitors are present in the normal adult human CNS and in the lesions of multiple sclerosis. *Brain* **121**, 2221–2228 (1998).
40. Wolswijk, G. Chronic stage multiple sclerosis lesions contain a relatively quiescent population of oligodendrocyte precursor cells. *J. Neurosci.* **18**, 601–609 (1998).
41. Wolswijk, G. Oligodendrocyte survival, loss and birth in lesions of chronic-stage multiple sclerosis. *Brain* **123**, 105–115 (2000).
42. Maeda, Y. *et al.* Platelet-derived growth factor-alpha receptor-positive oligodendroglia are frequent in multiple sclerosis lesions. *Ann. Neurol.* **49**, 776–785 (2001).
43. Chang, A., Tourtellotte, W.W., Rudick, R. & Trapp, B.D. Premyelinating oligodendrocytes in chronic lesions of multiple sclerosis. *N. Engl. J. Med.* **346**, 165–173 (2002).
44. van Heyningen, P., Calver, A.R. & Richardson, W.D. Control of progenitor cell number by mitogen supply and demand. *Curr. Biol.* **11**, 232–241 (2001).
45. Zhang, H. & Miller, R.H. Density-dependent feedback inhibition of oligodendrocyte precursor expansion. *J. Neurosci.* **16**, 6886–6895 (1996).
46. Nelson, P.J. & Daniel, T.O. Emerging targets: Molecular mechanisms of cell contact-mediated growth control. *Kidney Int.* **61**, 99–105 (2002).
47. Nimmerjahn, A., Kirchhoff, F. & Helmchen, F. Resting microglial cells are highly dynamic surveillants of brain parenchyma *in vivo*. *Science* **308**, 1314–1318 (2005).
48. Benediktsson, A.M., Schachtele, S.J., Green, S.H. & Dailey, M.E. Ballistic labeling and dynamic imaging of astrocytes in organotypic hippocampal slice cultures. *J. Neurosci. Methods* **141**, 41–53 (2005).
49. Bushong, E.A., Martone, M.E., Jones, Y.Z. & Ellisman, M.H. Protoplasmic astrocytes in CA1 stratum radiatum occupy separate anatomical domains. *J. Neurosci.* **22**, 183–192 (2002).
50. Thermes, V. *et al.* I-SceI meganuclease mediates highly efficient transgenesis in fish. *Mech. Dev.* **118**, 91–98 (2002).